

# The Application of Dyadic Wavelet In the RS Image Edge Detection\*

Qin Qiming Author1

Laboratory of Remote Sensing and GIS, Peking University, Beijing 100871, China;

[qmjin@pku.edu.cn](mailto:qmjin@pku.edu.cn)

Wang Wenjun Author2

Department of Electricity Engineering, Yanshan University, Qinhuangdao, Hebei, 066004, China;

[wwtingyan0662@sina.com](mailto:wwtingyan0662@sina.com)

Chen Sijin Author3

Laboratory of Remote Sensing and GIS, Peking University, Beijing 100871, China;

[dennis58220@263.net](mailto:dennis58220@263.net)

**Abstract:** In the edge detection of RS image, the useful detail losing and the spurious edge often appear. To solve the problem, we use the dyadic wavelet to detect the edge of surface features by combining the edge detecting with the multi-resolution analyzing of the wavelet transform. Via the dyadic wavelet decomposing, we obtain the RS image of a certain appropriate scale, and figure out the edge data of the plane and the upright directions respectively, then work out the grads vector module of the surface features, at last by tracing them we get the edge data of the object therefore build the RS image which obtains the checked edge. This method can depress the effect of noise and examine exactly the edge data of the object by rule and line. With an experiment of a RS image which obtains an airport, we certificate the feasibility of the application of dyadic wavelet in the object edge detection.

**Keywords:** Dyadic Wavelet, Remote Sensing Image, Edge Detection and Tracking, Object Recognition.

## 1. Introduction

In the RS image, the conventional filter methods often use the zero-crossing detection to examine the characteristic, but they often obtain some spurious edge when they face the special details such as a T junction

wavelet transform to deal with the RS image.

The wavelet analysis is a relatively new imaging tool that is rapidly developed from the Fourier transform, it has favorable localized character in the both spatial domain and frequency domain. The wavelet analysis consists of orthogonal wavelet, biorthogonal wavelet, dyadic wavelet, discrete wavelet and wavelet packets. Here we introduce dyadic wavelet to do edge detection. Dyadic wavelet [2] is a kind of wavelet between continuous wavelet and discrete wavelet, it has discrete scale parameters and continuous parameters in the spatial domain. So it has the same spatial-frequency covariational character as continuous wavelet which makes it important for the signal oddity detection and the edge detection.

The edges in an image can be divided into two groups: the step-edges and the roof-edges [3]. The gray levels of the image pixels on the two sides of the step-edge are totally different. The roof-edges are the points whose gray levels are from the increasing to the decreasing. It can be seen that the second order derivatives of the step-edges are zero-crossing and the second order derivatives of the roof-edges are the extrema. In order to use dyadic wavelet in the edge

detection, the wavelet is required to have linear displacement, in other words, dyadic wavelet must be zero-symmetrical. Therefore we could construct the

---

\* **Project (No. 40071061) supported by NSFC** and the trihedral vertices [1]. Here we introduce dyadic

zero-antisymmetrical and the zero-symmetrical dyadic wavelets[4].

If  $\varphi(t)$  is a mother dyadic wavelet,  $H(\omega)$  is the creating-atom,  $N$  is a random positive integer, array

$(a_1, a_2, \dots, a_N)$  satisfies  $\sum_{k=1}^N |a_k| < 1$ , we denote

${}_s\psi(t) \in L^2(R)$  as a zero-antisymmetrical dyadic

wavelet, then  ${}_s\psi(t)$  satisfies

$${}_s\hat{\psi}(2\omega) = {}_sG(\omega)\hat{\varphi}(\omega) \quad (1)$$

where  ${}_sG(\omega)$  is a high-pass filter for the structure of a zero-antisymmetrical dyadic wavelet

$${}_sG(\omega) = i \operatorname{sgn}(\omega) \left(1 + \sum_{k=1}^N a_N \cos k\omega\right) \sqrt{1 - |H(\omega)|^2} \quad (2)$$

If  $\varphi(t)$  is a mother dyadic wavelet,  $H(\omega)$  is the creating-atom,  $N$  is a random positive integer, array  $(a_1, a_2, \dots, a_N)$  satisfies  $\sum_{k=1}^N |a_k| < 1$ , we denote  ${}_c\psi(t) \in L^2(R)$  as a zero-symmetrical dyadic wavelet, then  ${}_c\psi(t)$  satisfies

$${}_c\hat{\psi}(2\omega) = {}_cG(\omega)\hat{\varphi}(\omega) \quad (3)$$

where  ${}_cG(\omega)$  is a high-pass filter for the structure of a zero-symmetrical dyadic wavelet

$${}_cG(\omega) = \left(1 + \sum_{k=1}^N a_N \cos k\omega\right) \sqrt{1 - |H(\omega)|^2} \quad (4)$$

Therefore we get two filters for the structures of dyadic wavelets  ${}_sG(\omega)$  and  ${}_cG(\omega)$ , where  ${}_sG(\omega)$

is an odd function,  ${}_cG(\omega)$  is an even function,

$${}_sG(\omega) = \sum_{n \in Z} {}_s g_n e^{-in\omega} \quad (5)$$

$${}_cG(\omega) = \sum_{n \in Z} {}_c g_n e^{-in\omega} \quad (6)$$

## 2. Edge Detection and Tracking of Images

In the dyadic wavelet decomposition of an image we

should determine three filters: where  $H(\omega)$  is the

creating-atom of the mother dyadic wavelet,  $G(\omega)$  is

just defined in Eq.(5) and Eq.(6),  $L(\omega)$  is a low-pass

filter such that

$$L(\omega) = \frac{1}{\sqrt{2}} \left(1 + \sum_{k=1}^N b_k \cos k\omega\right) \sqrt{1 + |H(\omega)|^2} \quad (7)$$

where array  $(b_1, b_2, \dots, b_N)$  satisfies  $\sum_{k=1}^N |b_k| < 1$ . Then

we could define  $\hat{\varphi}(2w), \hat{\psi}(2w), \hat{\xi}(2w)$

$$\hat{\varphi}(2w) = H(w)\hat{\varphi}(w)$$

$${}_c\hat{\psi}(2w) = {}_cG(w)\hat{\varphi}(w), {}_s\hat{\psi}(2w) = {}_sG(w)\hat{\varphi}(w) \quad (8)$$

$$\hat{\xi}(2w) = L(w)\hat{\varphi}(w)$$

At last we obtain the smooth function in two dimensions:

$$\varphi(x, y) = \varphi(x)\varphi(y) \quad (9)$$

$$\hat{\varphi}(\omega_x, \omega_y) = \hat{\varphi}(\omega_x)\hat{\varphi}(\omega_y) \quad (10)$$

and the zero-antisymmetrical functions in two dimensions:

$${}_s\psi^1(x, y) = {}_s\psi(x)\xi(y) \quad (11)$$

$${}_s\psi^2(x, y) = {}_s\psi(y)\xi(x) \quad (12)$$

and the zero-symmetrical functions in two dimensions:

$${}_c\psi^1(x, y) = {}_c\psi(x)\xi(y) \quad (13)$$

$${}_c\psi^2(x, y) = {}_c\psi(y)\xi(x) \quad (14)$$

The figure of dyadic wavelet decomposition in two dimensions [5] is:

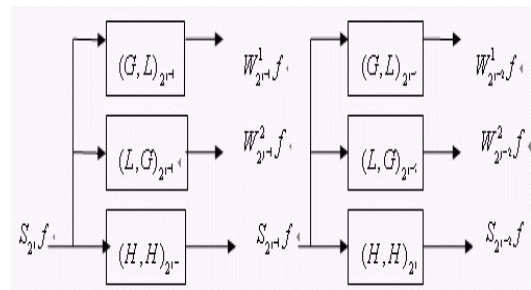


Fig1 dyadic wavelet decomposition in two levels

where  $S_{2^j} f(x, y)$  is the portion which is smoothed both in the plane and upright directions after being

decomposed in the level  $j$ ,  $W_{2^j}^1 f(x, y)$ ,  $W_{2^j}^2 f(x, y)$  are the edge information in the plane and upright directions respectively. In each scale, edge information expresses the local module maxima which mean the gradient vector module maxima. The gradient vector module is  $M_{2^j} f(x, y) = \sqrt{(W_{2^j}^1 f)^2 + (W_{2^j}^2 f)^2}$ , and

$$A_{2^j} f(x, y) = \arctan\left(\frac{W_{2^j}^2 f}{W_{2^j}^1 f}\right)$$
 is the gradient vector angle.

So it is clear that edge information is the points which are the gradient module maxima in the gradient vector angle direction.

In case of a plane image  $f(x, y)$  (Fig.2) we use dyadic wavelet to decompose in one level ( $j = 1$ ), after computing  $S_2 f(x, y) = \sum_{l \in Z} \sum_{k \in Z} h_l h_k S f(x-l, y-k)$ , we get the smooth portion of the image (Fig.3).



Fig.2. A plane image



Fig.3. The smoothed image

After computing

$$W_2^1 f(x, y) = \sum_{l \in Z} \sum_{k \in Z} g_l l_k S f(x-l, y-k),$$

$$W_2^2 f(x, y) = \sum_{l \in Z} \sum_{k \in Z} l_l g_k S f(x-l, y-k),$$
 we get the

images depicting the edge information of the plane direction (Fig.4) and the upright direction (Fig.5) respectively.



Fig.4. The plane edge image



Fig.5. The upright edge information

By computing the gradient vector module

$M_{2^j} f(x, y) = \sqrt{(W_{2^j}^1 f)^2 + (W_{2^j}^2 f)^2}$ , we get the edge of the image (Fig.6).

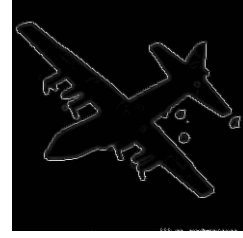


Fig.6. The edge image

Now we had got the edges of an image by computing the gradient vector module of some certain scale after dyadic wavelet decomposition. But this time the edges contain some inconsecutive points and spurious edges. So the edge tracking is needed. The edge tracking is to connect the discontinuous edge points together to a close boundary. The process fills up the clearance which is produced by noise and the shadow. Here we propose a new best-path method to track the edges. The method is:

- 1) Mark the coordinate  $A(x, y)$  of the edge point A which is in the top left corner of the gradient vector module image, then use A as the center open a window whose size is  $30 \times 30$ . If both coordinates of A are less than the default threshold (such as 30), then let the smaller of  $x$  and  $y$  as the radius of the window, and mark A.
- 2) In the window, from the plane direction, ascertain counter-clockwise the detected edge point which is nearest the center and not marked. Then let the point as the center B of the next window, if A and B are 8-adjacent, then mark B, otherwise, we should ascertain the best path between A and B.
- 3) The best path between A and B is ascertained in this step. The path should be along the gradient direction of A and B, and the number of the path points should be the least. Then mark the path points as A and B.
- 4) After ascertaining B, let B as the start point, repeat 1), 2), 3) until goes back to A. Therefore we get the whole edge.

#### 4. The Experiment of Edge Detection and Discussion

Here we use the dyadic wavelet to detect the edges of an airport image in various scales to find a best scale for the detection. The airport image is Fig.7.

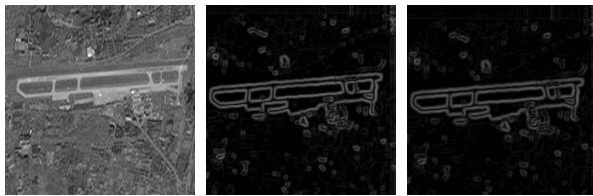


Fig.7. The airport image Fig.7-1

Fig.7-2



Fig.7-3

Fig.7-4

Fig.8-1

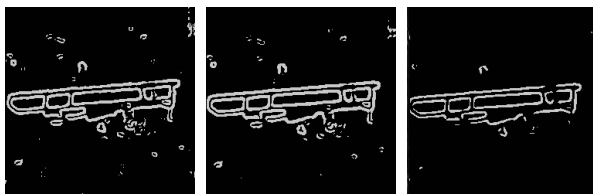


Fig.8-2

Fig.8-3

Fig.8-4

Fig.7-1,7-2,7-3 and 7-4 are the gradient vector module of original image Fig.7 after dyadic wavelet decomposition for four, five, six and seven layers respectively. Doing edge tracking of these images by the method introduced above we get Fig.8-1,8-2,8-3 and 8-4. Since dyadic wavelet has discrete scale parameters and continuous parameters in the spatial domain, when dyadic wavelet decompose the image for  $j$  levels, the scale is  $2^j$ , so the outcomes of different scales are the embodiment of multi-resolution. From the decomposed image, the resolution is decrease when the scale is increase, at the same time, noise is restrained apparently. Meanwhile, some detail is lost in result of the increasing scales, therefore lead the detected edge incomplete and the position of the edge inaccurate. Moreover when the scale is small, the influence of noise is undeniable. So it is valuable to get the suitable scale to not only restrain noise effectively but also detect the edge accurately. Here we decompose the image for six layers(Fig.7-3), and use the method mentioned above to track the edge(Fig.8-3).

From the result of the experiment, we find that it is

feasible for dyadic wavelet to detect the edges of RS images and solve problem of both straining noise and localizing edges. Especially, some details such as T junction and the trihedral vertices can be detected accurately, and there is almost no spurious edge. The key of the application of this method is to choose a most suitable scale according to the character of the image in order to detect the edge accurately without losing essential detail and restrain noise as well. In a certain suitable scale, dyadic wavelet can detect the specific diversification of the image edge character, and with our edge tracking method, we can connect the edges into a close curve which provides the foundation for the further researches such as object recognition.

## References

- [1] E. De Micheli, Localization and Noise in Edge Detection IEEE *Trans. Patt. Anal. Machine Intell.*, Vol. PAMI-11. pp1106-1117. 1989
- [2] Peng Yu-hua, Wavelet transform and engineering application, Science press, p.33
- [3] Liu Liudi, Liu Mingqi, Practical digital image processing, Beijing institute of technology press, p.180
- [4] Xu Chuanxiang, Shi Qingyun and Cheng Minde, Zero-symmetrical and zero-antisymmetrical dyadic wavelet and its application to edge detection, *China journal of image and graphics*, Vol.1, No.1, May, pp4-11, 1996
- [5] Stephane Mallat, Sifen Zhong Characterization of Signals from Multiscale Edges. *Trans. Patt. Anal. Machine Intell.*, Vol. 14, No.7, pp. 710-732. 1992.